

Electronic Supplementary Information (ESI)

**Improved Neuromorphic Functionality in Organic Electrochemical Transistors Using
Crosslinked-Polyvinyl alcohol for Fast Ion Transport and its Application to Pavlovian
Transistors**

Seung Hwan Song^{1,4}, Jeong Hye Song^{1,4}, Jisoo Park^{2,4}, Hocheon Yoo^{3,*}, and Eun Kwang Lee^{1,*}

¹*Department of Chemical Engineering, Pukyong National University, Busan 48513, Republic of Korea*

²*Department of Semiconductor Engineering, Gachon University, Seongnam 13120, Republic of Korea*

³*Department of Electronic Engineering, Hanyang University, 222 Wangsimni-ro, Seoul 04763,
Republic of Korea*

⁴ *These authors contributed equally to this work*

* Corresponding author

Email address: hocheon@hanyang.ac.kr (H. Yoo), eklee@pknu.ac.kr (E. K. Lee)

Keywords: Organic Electrochemical Transistor; Cross-linking; Ion Transport; Synaptic Plasticity; Neuromorphic Computing

Table S1. Summary table of previously reported OECTs for material, key electrical parameter, and synaptic plasticity demonstration.

Channel	Electrolyte	μC^* (F V ⁻¹ s ⁻¹ cm ⁻¹)	$g_{m, \text{max}}$ (mS)	I_{on}/I_{off}	Synaptic plasticity	Year	Ref.
PE ₂ -OE ₄	NaCl	831	15.36	1 x 10 ³	N/A	2025	⁵⁸
PEDOT: PSS	PVDF-TrFE / BMIM:TFSI	496	0.4	151	LTP	2025	⁵⁹
PEDOT: PSS	MTEOA: MeOSO ₃	284	7.766	8.12×10^4	N/A	2022	⁶⁰
P3HT: APT	BMIM:TFSI / PVDF-TrFE	67	1.27	5.82×10^4	LTP	2024	⁶¹
DPPDTT -p-ps	PBS	1103	10.8	10^4	LTP	2025	⁶²
CX- P3HT	TFSI	41.33	1.67	5.9×10^3	LTP, LTD	2024	³⁰
CX-PVA / CX- P3HT	BMIM:TFSI	206	0.3229	2.5×10^3	LTP, LTD	2025	This work

References in Table S1:

- 30. S. M. Park, Y. Won, J. H. Oh and E. K. Lee, *Adv. Mater. Technol.*, 2024, **10**, 2401316
- 58. O. Bardagot, B. T. DiTullio, A. L. Jones, J. Speregen, J. R. Reynolds and N. Banerji, *Adv. Funct. Mater.*, 2025, **35**, 2412554.
- 59. Y. J. Lee, Y. H. Kim and E. K. Lee, *Macromol. Rapid Commun.*, 2024, **45**, 2400165
- 60. T. Li, J. Y. Cheryl Koh, A. Moudgil, H. Cao, X. Wu, S. Chen, K. Hou, A. Surendran, M. Stephen, C. Tang, C. Wang, Q. J. Wang, C. Y. Tay and W. L. Leong, *ACS Nano*, 2022, **16**, 12049–12060
- 61. D. H. Kim, J. Lee, Y. Kim, H. Yoo and E. K. Lee, *Org. Electron.*, 2024, **131**, 107076.
- 62. X. Yang, X. Chen, P. Gu, Z. Hu, X. Zhang, Z. Sun, L. Lu, G. Zu and J. Huang, *Biomaterials*, 2025, **322**, 123416.

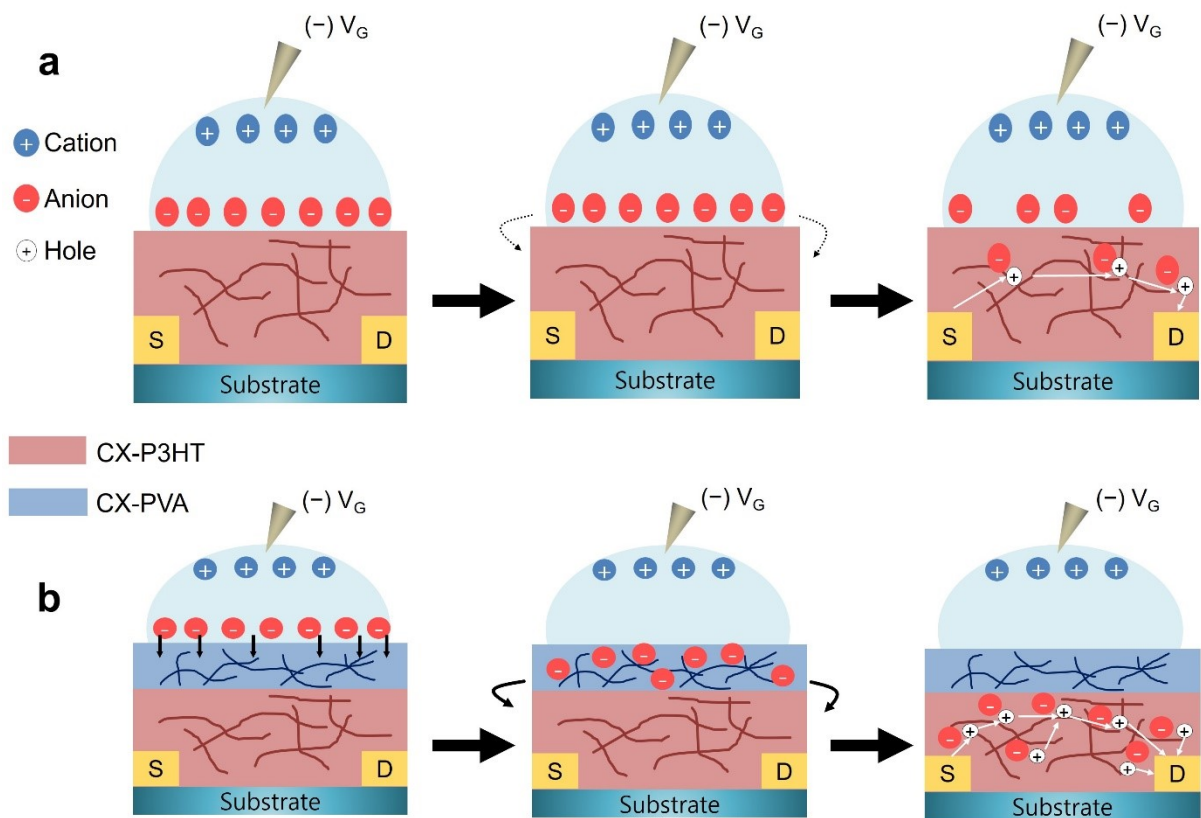


Fig. S1. The process of current flow a) only the CX-P3HT film, b) both CX-P3HT and CX-PVA films.

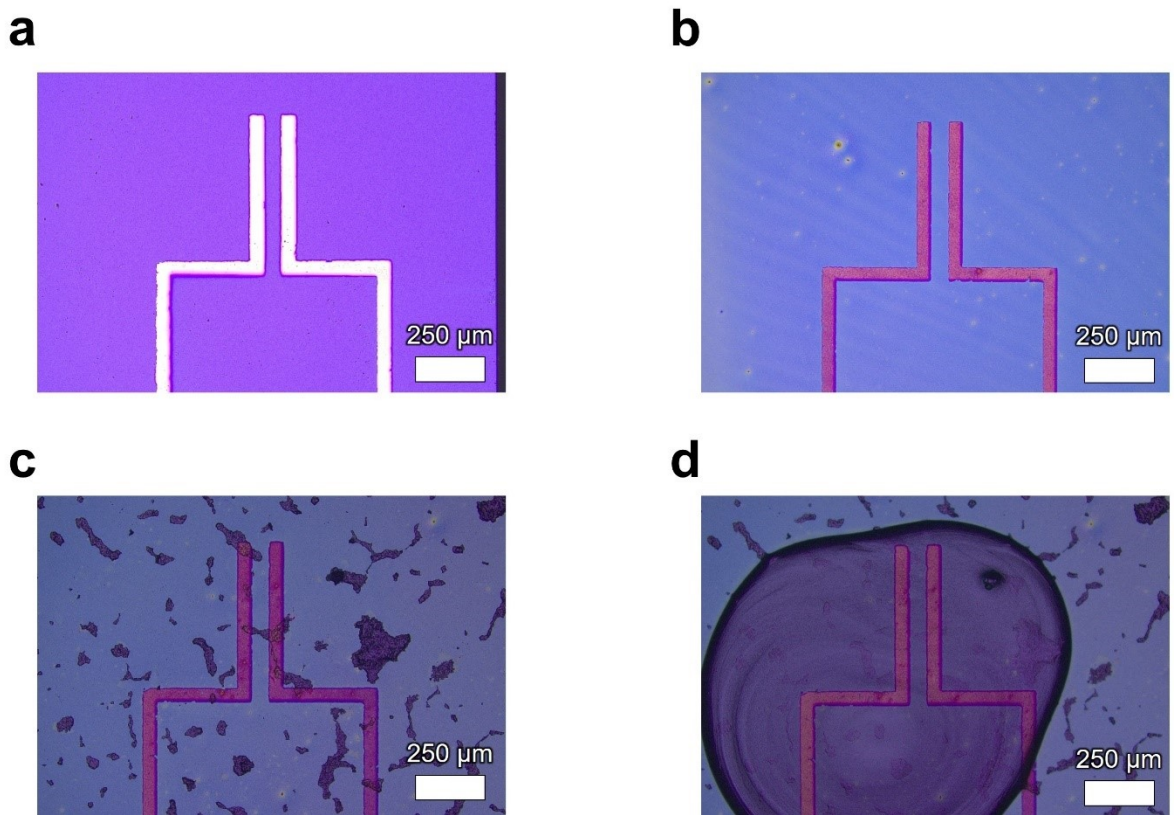


Fig. S2. OM images of each fabrication step of the device a) formation of source and drain electrodes using chromium and gold, b) formation of the CX-P3HT film, c) formation of the CX-PVA film, and d) deposition of the BMIM:TFSI ion gel.

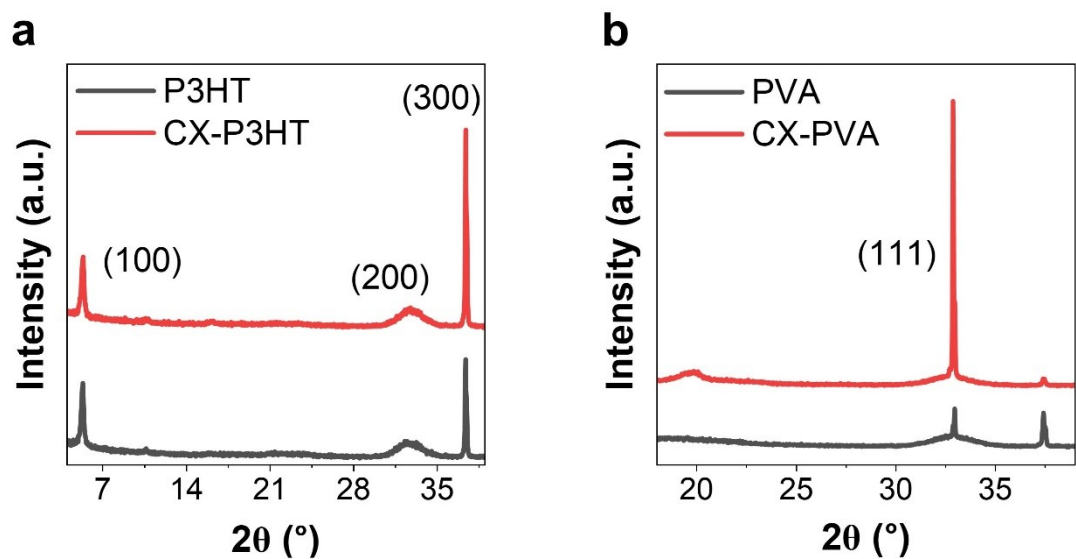


Fig. S3. XRD pattern of the device a) with only the CX-P3HT film, b) with both CX-P3HT and CX-PVA films.

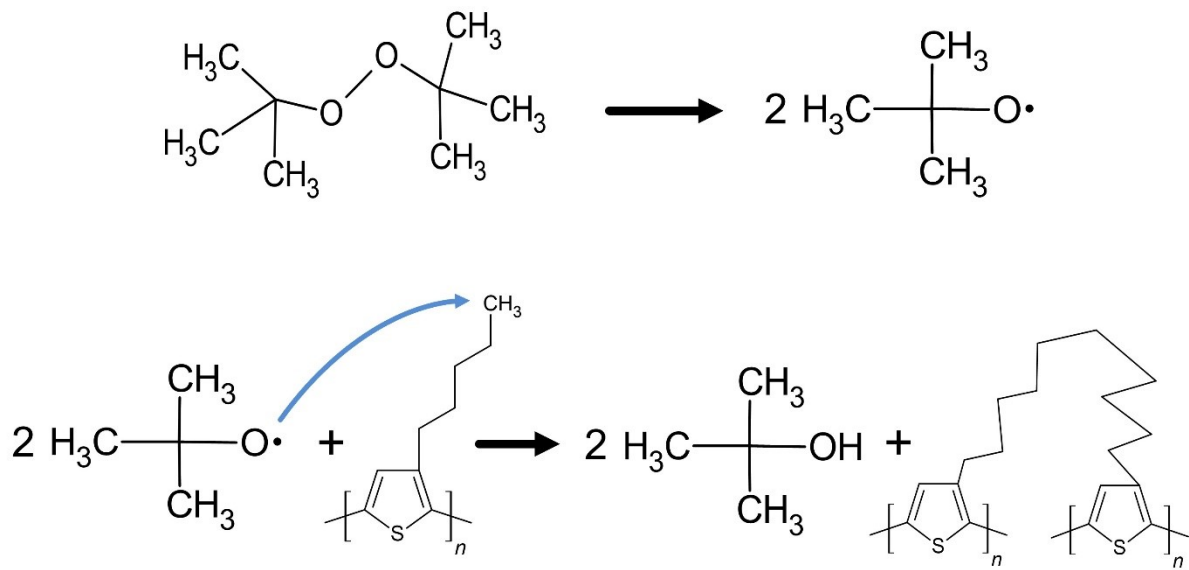


Fig. S4. The crosslinking reaction mechanism of the crosslinking agent DTBP and P3HT.

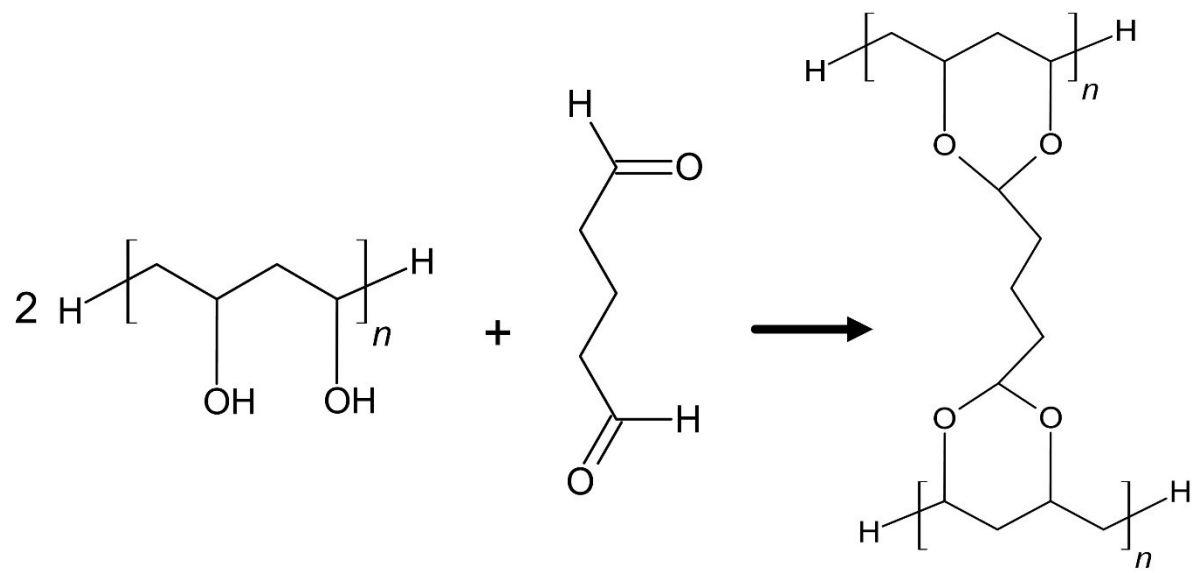


Fig. S5. The crosslinking reaction mechanism of the crosslinking agent glutaraldehyde and PVA.

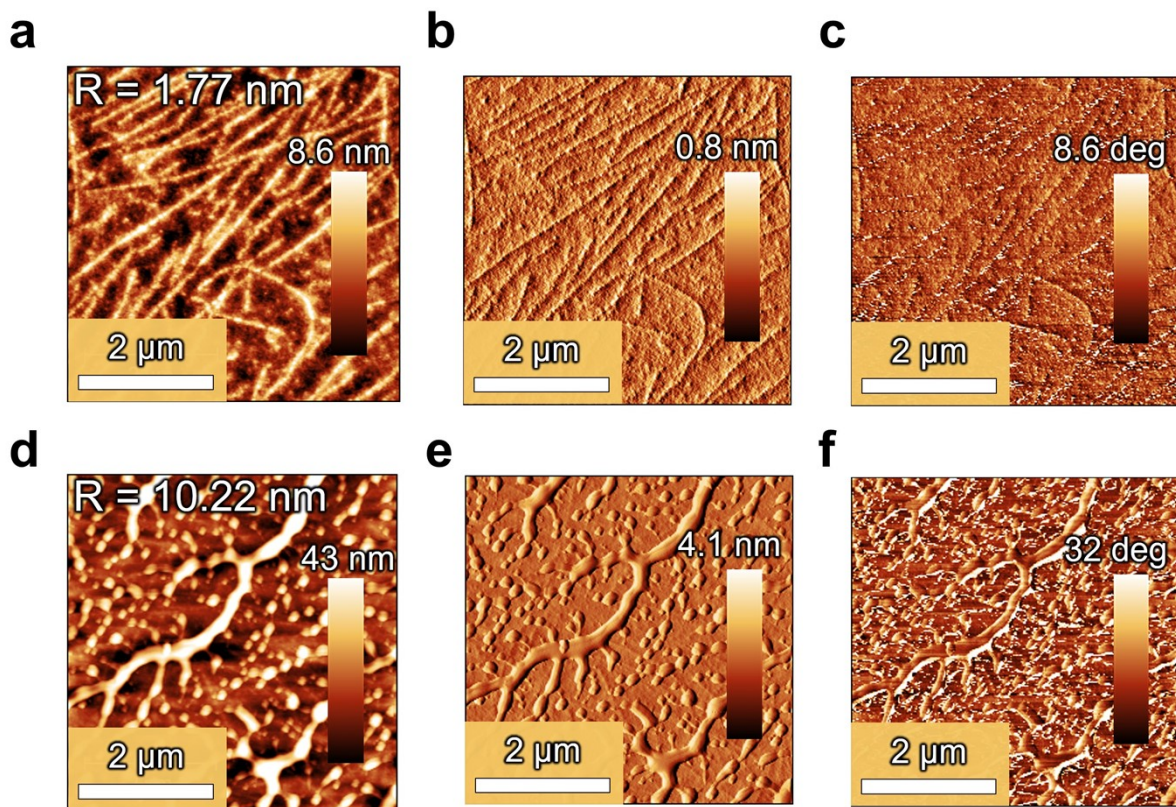


Fig. S6. AFM images of a, b, c) only the CX-P3HT film: height, amplitude, and phase. d, e, f) Both CX-P3HT and CX-PVA films: height, amplitude, and phase.

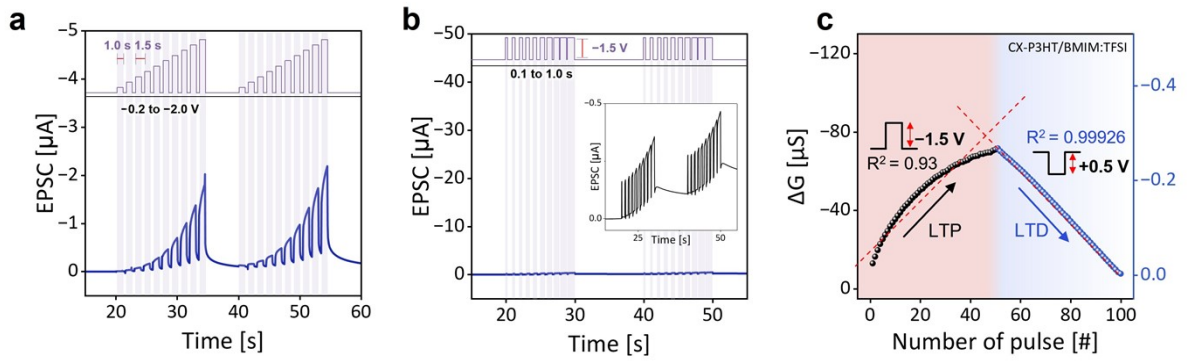


Fig. S7. Only the CX-P3HT film is present a) pulse voltage, b) pulse width, c) LTP and LTD performance.

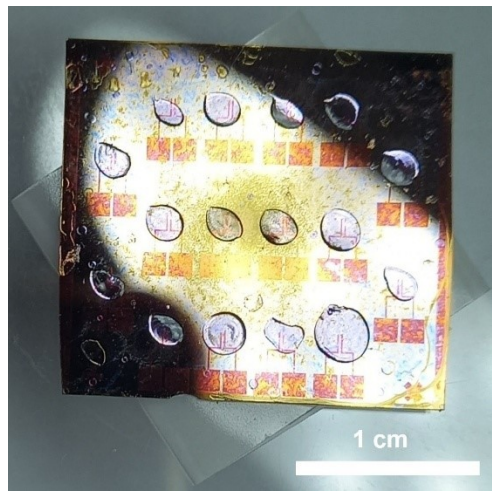


Fig. S8. Array integration of 16 CX-P3HT/CX-PVA devices.

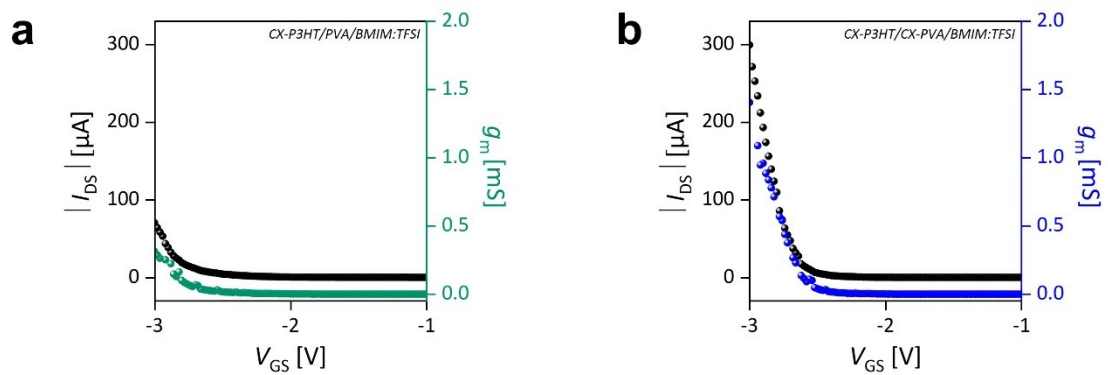


Fig. S9. Transfer and transconductance curves of a) the CX-P3HT/pure PVA device, b) the CX-P3HT/CX-PVA device.

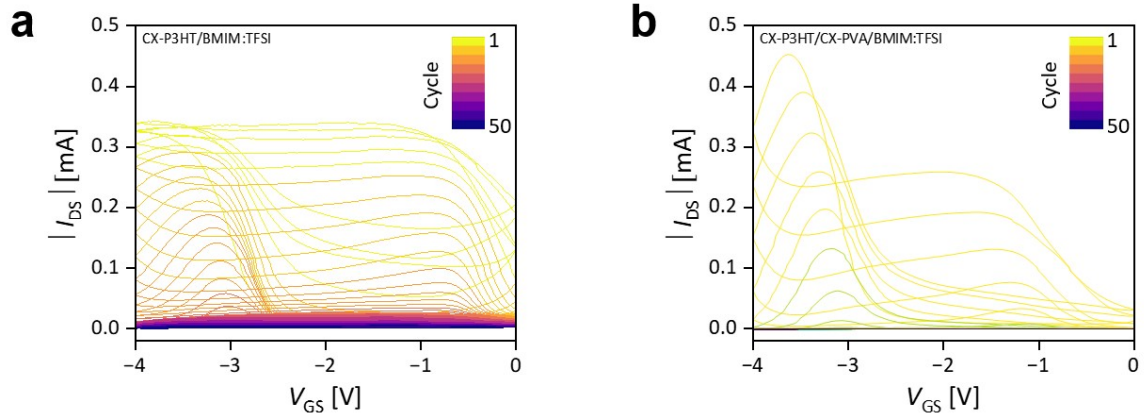


Fig. S10. Transfer curves over 50 cycles for a) the CX-P3HT-only device, b) the CX-P3HT/CX-PVA device.

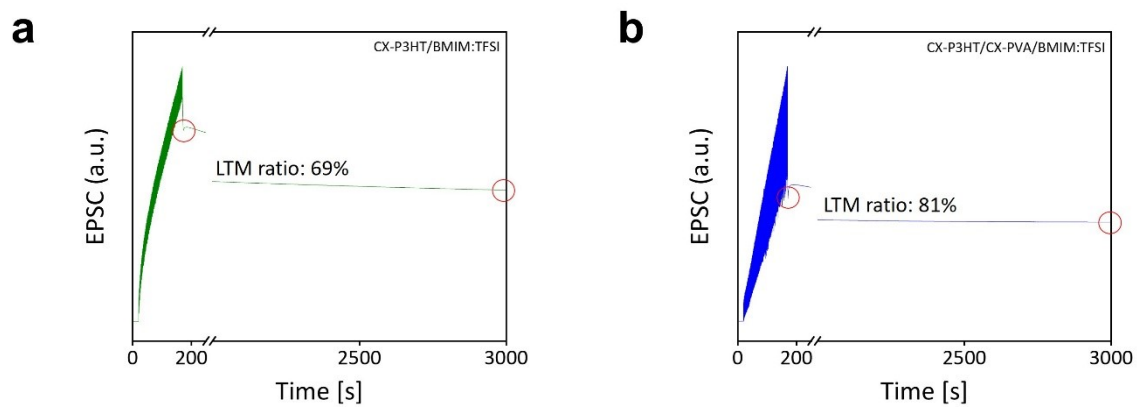


Fig. S11. LTM trends for a) the CX-P3HT-only device, b) the CX-P3HT/CX-PVA device.

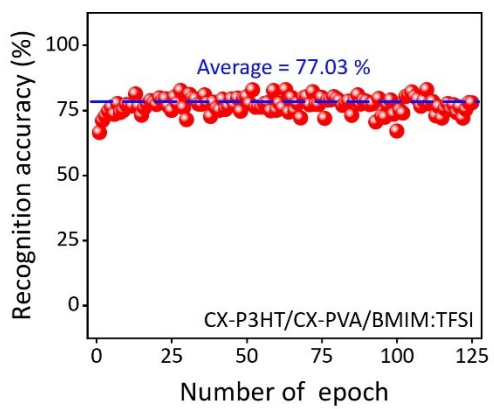


Figure S12. Recognition accuracy as a function of epochs for CX-P3HT OECT with CX-PVA film.